Int J Thermophys (2018) 39:30
https://doi.org/10.1007/s10765-017-2350-3

# Evaluation of Building Energy Saving Through the Development of Venetian Blinds' Optimal Control Algorithm According to the Orientation and Window-to-Wall Ratio

**Hyuk Ju Kwon[1] · Sang Hun Yeon[1] · Keum Ho Lee[2] · Kwang Ho Lee[1]**

Received: 12 September 2017 / Accepted: 22 December 2017 / Published online: 4 January 2018


**Abstract** As various studies focusing on building energy saving have been continuously conducted, studies utilizing renewable energy sources, instead of fossil fuel, are needed. In particular, studies regarding solar energy are being carried out in the field of building science; in order to utilize such solar energy effectively, solar radiation being brought into the indoors should be acquired and blocked properly. Blinds are a typical solar radiation control device that is capable of controlling indoor thermal and light environments. However, slat-type blinds are manually controlled, giving a negative effect on building energy saving. In this regard, studies regarding the automatic control of slat-type blinds have been carried out for the last couple of decades. Therefore, this study aims to provide preliminary data for optimal control research through the controlling of slat angle in slat-type blinds by comprehensively considering various input variables. The window area ratio and orientation were selected as input variables. It was found that an optimal control algorithm was different among each window-to-wall ratio and window orientation. In addition, through comparing and analyzing the building energy saving performance for each condition by applying the developed algorithms to simulations, up to 20.7 % energy saving was shown in the cooling period and up to 12.3 % energy saving was shown in the heating period. In addition, building energy saving effect was greater as the window area ratio increased given the same orientation, and the effects of window-to-wall ratio in the cooling period were higher than those of window-to-wall ratio in the heating period.

✉ Kwang Ho Lee
kwhlee@hanbat.ac.kr

1 Graduate School, Department of Architectural Engineering, Hanbat National University, San 16-1, Dukmyung-Dong, Yuseong-Gu, Daejeon 305-719, Korea

2 Green Energy Institute, 177, Samhyangcheon-ro, Mokpo-si, Korea

**Keywords** Building energy · EnergyPlus · Orientation · Slat angle · Venetian blind · Window-to-wall ratio

## 1 Introduction

### 1.1 Background and Purpose of Study

As various studies focusing on building energy saving have been continuously conducted, studies utilizing renewable energy sources, instead of fossil fuel, are needed. In particular, solar energy among various green energies is an infinite energy source with no regional limitation unlike fossil fuel; studies to utilize solar energy actively have been continuously undertaken in the field of construction. In order to utilize such solar energy effectively, solar radiation transmittance into buildings should be controlled properly. The window which is the only exterior element in buildings that can allow solar penetration can be effectively utilized to control the amount of solar radiation transmittance for the minimized lighting, heating and cooling energy, while maintaining visual comfort. However, since the glass skin cannot control the solar radiation by itself due to its material characteristics as a glazing material, auxiliary solar radiation control devices which can control indoor thermal and light environments are required [1]. Blinds are currently a typical solar radiation control device for the glass skin. Venetian blinds enable the control of slat angle by acquiring and blocking solar radiation in a balanced manner, giving a positive effect on indoor thermal and light environments. However, venetian blinds are generally controlled manually by a subjective judgment of indoor occupants, which is not an efficient way to reduce the building energy through the streamlined control of venetian blinds and thus it should also be resolved. According to on-site investigation of operation status of blinds at office buildings, it was found that blinds were not controlled properly due to excessive work schedule of the occupants and most blinds were maintained in the closed state [2]. Rational control is impossible from such manual control due to practical conditions of indoor occupants; studies regarding automatic control of venetian blinds as a control method have been carried out for improving energy saving performance in buildings.

In a related study, H. Burak Gunay et al analyzed the lighting power and blind adjustment behavior in ten private offices along with real-time solar irradiance, work space illuminance, and occupancy data to quantitatively evaluate the relationship among those accumulated data. Upon this analysis, an adaptive lighting and blinds control algorithm was formulated. The results indicate that the use of an adaptive lighting and blinds control algorithm developed in this paper can substantially reduce the lighting loads in office buildings without adversely affecting the occupant comfort [3]. Kwang Gyu-min et al proposed the cooperative control coupled with heating, cooling, lighting and blind control system to minimize the energy use in buildings. The blind condition is optimized to minimize the total energy of heating, cooling and lighting. The results show that the proposed control system reduces the cooling energy demand by about 40.8 % and 19.6 % of the lighting energy compared to the conventional control system with maintaining the same thermal comfort level [4]. Zhijin chen et al

presented various lighting and blind control methods to improve user comfort and reduce energy consumption simultaneously. They introduced an improved reinforcement learning controller to obtain an optimal control strategy of blinds and lights. The proposed system was implemented on a practical test-bed in an energy-efficient building. Compared with the traditional control, it can provide a more acceptable and energy-efficient luminous environment [5]. In addition, Oh Myung-Hwan defined control-related variables as surface solar radiation, developed an optimal control algorithm where building energy and visual comfort through a change in slat angle were comprehensively considered, and analyzed building energy performance when the developed algorithm was applied [6]. Hu et al. developed an illuminance-based slat angle selection (ISAS) model that predicts the optimum slat angles of split blinds to achieve the designed indoor illuminance, based on a series of multi-layer feed-forward artificial neural networks (ANNs). The illuminance values at the sensor points used to develop the ANNs were obtained by EnergyPlus, and the model was validated by evaluating the errors in the calculation of the: (1) illuminance and (2) optimum slat angles [7]. Furthermore, Reinhart suggested the artificial lighting control integrated with the blind control. Occupancy profile and workstation illuminance level have been plugged in as the input condition in the control algorithm and improved energy efficiency could be achieved compared to the manual blind control. However, the study mainly focused on the lighting energy reduction and thus the total building energy and the occupant visual comfort have not been taken into account [8]. Park Young-joon et al carried out an experimental analysis to compare the energy consumption between automatically controlled blinds and manually controlled blinds targeting the cooling period. Under the assumption that automatically controlled blinds were close and manually controlled blinds were open, it was found that when lighting control was not considered, the cooling load was reduced, but when lighting was considered, there was no significant difference in the energy consumption [9]. Many studies related to optimized blind control have been carried out, but most of those studies focus on building energy saving under the condition of a certain orientation and a fixed window-to-wall ratio in the optimized blind control strategy. However, such results under the condition of a specific orientation and window-to-wall ratio are not enough to be generalized for optimized blind control; and a proper optimized blind control strategy according to various input variables is necessary.

Therefore, this study intended to specifically consider outdoor environment and building characteristics when properly controlling venetian blind. This study is a follow-up study of Myung-Hwan Oh's master's thesis [6], but the window orientation and window-to-wall ratio having significant effects on indoor thermal and visual environments were additionally considered as control variables. In addition, the building energy saving performance was compared and analyzed by applying the optimal control algorithms developed according to different orientations and window-to-wall ratios to simulations. The purpose of this study is to provide preliminary data for optimal control research through the controlling of slat angle in venetian blinds by comprehensively considering various input variables.

### 1.2 Method and Scope of Study

In this study, an optimized venetian blind control strategy was established by modeling a virtual office building where blinds were installed. The optimal control strategy used in this study is the development of a control algorithm through the control of slat angle. The overall slow chart of this study is illustrated in Fig. 1. A theoretical analysis method using a simulation tool was used in order to develop an optimal control algorithm which varied according to various input variables, and the development method proven in previous studies [6] was used. The optimized slat angle for developing an algorithm was defined as the minimized building energy (cooling + heating + lighting); and lighting energy saving through lighting dimming control to meet 500 lux as the minimum indoor illumination intensity was also considered. In addition, the blinds used in this study were internal venetian blinds with horizontal slats of which reflectance was constantly fixed at 0.9, and the simulation was carried out by applying an angle between 0° and 90° for the slat angle. The input variables applied in this study included the orientation and the window-to-wall ratio that were important elements in the thermal behavior of window; and a different optimal control algorithm was developed for each orientation (East, West, South, North) and each window-to-wall ratio (33 %, 50 %, 70 %) condition. In addition, optimal control algorithms were developed for the cooling period (June, July, August) and the heating period (December, January, February), respectively; and a comparative analysis of building energy (cooling + heating + lighting) saving performance was carried out by applying the different optimal control algorithms developed for each condition to the simulation.

## 2 Theoretical Background

### 2.1 Selection of Simulation Tool

EnergyPlus v6.0 developed by the U.S. Department of Energy was used as a theoretical analysis tool to conduct this study. EnergyPlus is the program combining the advantage of DOE-2 in the system analysis and the advantage of BLAST in the load analysis [10]. In addition, the building cooling and heating load analysis was based on the heat balance method recommended by the American Society of Heating Refrigerating and Air-conditioning Engineer (ASHRAE). The credibility of this program was verified by developing simulation tools as per the ASHRAE 140 guidelines which were the representative dynamic simulation protocol [11,12]. In addition, the heat flow such as solar radiation, longwave radiation, and shortwave radiation was able to be calculated on building skins; and the calculation of heat flow entering into the indoors through venetian blinds utilized in this study and the detailed calculation of indoor load using the equation of thermal equilibrium were also available [13]. In addition, detailed information on the assumptions, detailed algorithm and validation of EnergyPlus models related to windows, blinds and day-lighting calculations can also be found in [13].

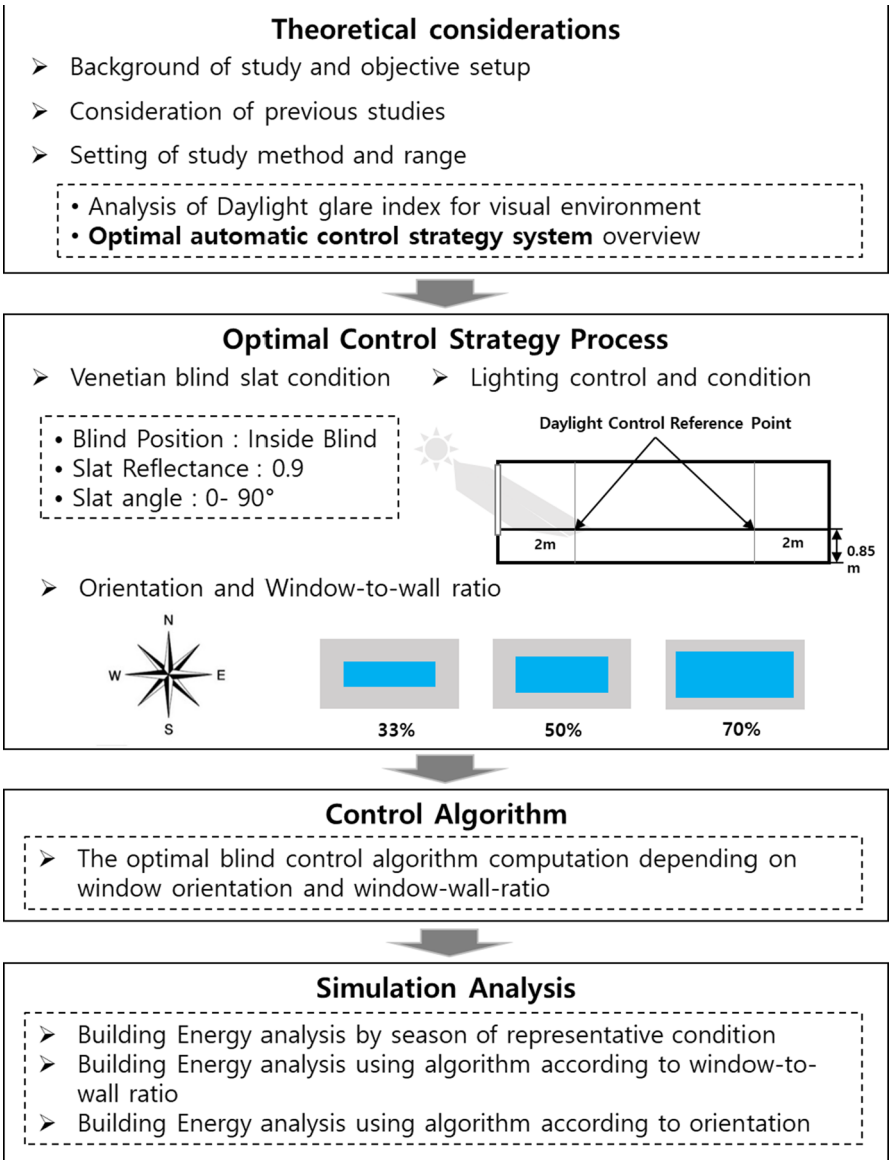


**Fig. 1** Study flowchart

## 2.2 Theoretical Background of Solar Radiation Transmittance and Absorption Rate of Window

There are two methods to deliver solar energy into the indoors directly through windows where venetian blinds are applied: the penetration in the forms of direct solar radiation and diffused solar radiation, and the inflow of solar radiation in the forms

**Table 1** Separation of solar radiation transmittance and reflectance in blind slats

| Terms | Explanation |
|---|---|
| $\tau_{dir,dif}$ | Direct-to-diffuse transmittance (same for front and back of slat) |
| $\tau_{dif,dif}$ | Diffuse-to-diffuse transmittance (same for front and back of slat) |
| $\rho^{f}_{dir,dif}, \rho^{b}_{dir,dif}$ | Front and back direct-to-diffuse reflectance |
| $\rho^{f}_{dif,dif}, \rho^{b}_{dif,dif}$ | Front and back diffuse-to-diffuse reflectance |

of shortwave and longwave. In order to analyze such characteristics mathematically, the EnergyPlus analysis tool was used to perform a numerical analysis based on the theoretical analysis method from the research result "Solar radiation transport through venetian blinds" published by Simmler, Fischer and Winkelmann in 1996. In the determination of optical characteristics, the internal reflection in a space between the slat and the glass is ignored, and the slat composition, subsequently, has a great effect on the analysis of solar radiation behavior on windows where venetian blinds are applied. Therefore, it is necessary to understand the mathematical theory regarding the effects of slat composition on the optical characteristics and the process that solar energy is delivered into the indoors through the penetration of solar energy and the inflow of solar radiation [6,13].

At first, in order to identify the optical characteristics of blinds, data of solar radiation transmittance and reflectance in blind slats are required as shown in Table 1. At this time, $\tau_{dir,dir} = 0$, $\rho^{f}_{dir,dif} = 0$ and $\rho^{b}_{dir,dif} = 0$ are established, as a result of solar radiation coming into contact with the slat and not becoming the direct solar radiation under the condition of assumption that the slat is the perfectly diffusing surface. In addition, the transmittance and reflectance of solar radiation change according to the slat angle and the incidence angle of solar radiation. For the intensive mathematical calculation of such effects, it is assumed in EnergyPlus that the transmittance and reflectance data of direct solar radiation and diffused solar radiation are the same as $\tau_{dir,dif} = \tau_{dif,dif}$, $\rho^{f}_{dir,dif} = \rho^{f}_{dif,dif}$ and $\rho^{b}_{dir,dif} = \rho^{b}_{dif,dif}$. The form of solar radiation brought into the indoors from the outside is classified into direct solar radiation and diffused solar radiation. The direct transmittance of direct solar radiation occurs when solar radiation is brought into the indoors directly without coming into contact with the slat as shown in Fig. 2a, and it can be expressed as the following equation [6,13].

$$\tau_{dir,dif} = 1 - \frac{|\omega|}{h}, \ |\omega| \le h, \ \omega = \mathrm{s}\frac{\cos(\varphi_b - \varphi_s)}{cos\varphi_s} \tag{1}$$

The inflow of direct solar radiation in the form of diffused solar radiation can be analyzed through six divided slat sections as shown in Fig. 3-1b: s1 is the section where direct solar radiation is directly brought in, s2 is the section where actual diffused solar radiation is brought in between the slats after calculating the penetration, reflection and absorption, s3 and s4 are the sections where direct solar radiation is reflected directly from the slat, and s5 and s6 are the sections where direct solar radiation is indirectly reflected. In this regard, it is to determine the inflow rate of direct solar

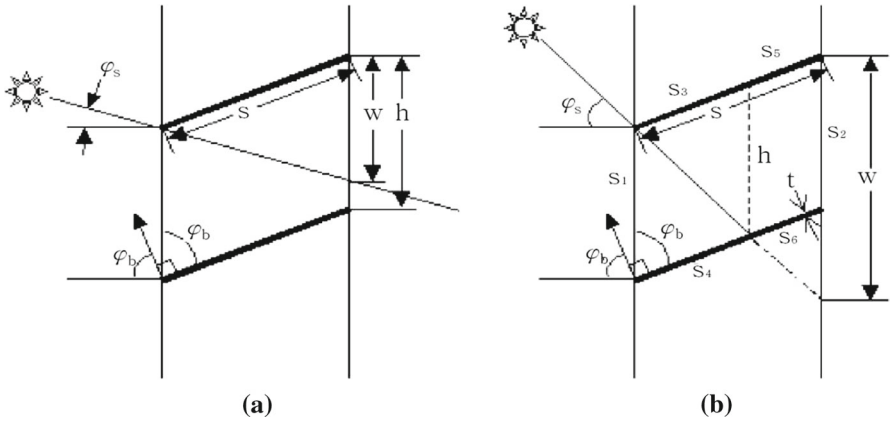


**Fig. 2** Inflow of external direct sunlight in the space between blinds slat (a) direct-to-direct blind transmittance; (b) direct-to-diffuse blind transmittance [13]

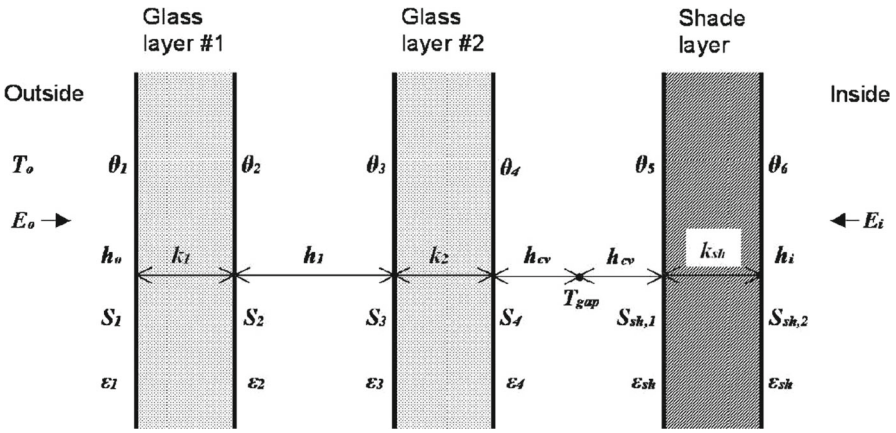


**Fig. 3** Heat transfer in dual window system with internal blind [13]

radiation diffused to s2 due to a physical phenomenon between the slats, after the direct solar radiation has passed through s1. It can be seen that to determine the diffused transmittance in EnergyPlus, radiosity method, which accumulates optical energy from the light source on each divided side, exchanges reflected energy, and calculates repeatedly until the amount of energy is balanced, is used. In order to utilize such radiosity method, each divided side is classified and the diffuse transmittance of direct solar radiation is calculated repeatedly using an analysis equation such as equation (2) according to 3 vector quantities and the angle factor to find the value [6,13].

$J_i$: the radiosity of segment si, "i.e.," the total radiant flux into the cell from si
$G_i$: the irradiance on the cell side of si
$Q_i$: the source flux from the cell side of si
$F_{ji}$: the view factor between sj and si

$$G_i = \sum_{j=1}^{6} J_j F_{ij}, \quad i = 1, 6 \tag{2}$$

### 2.3 Theoretical Background of Heat Transfer and Air Flow Between Internal Blinds and Windows

A proven analysis theory for heat transfer according to an increase in the surface temperature of the slat and air flow due to an increase in the ambient air temperature, in addition to the solar radiation behavior on windows where blinds are installed mentioned earlier, is necessary. EnergyPlus can interpret the internal and external blinds on windows and the blinds in the intermediate space, and it can also analyze radiation, conductive and convective components in the heat transfer between glass, blinds and the indoors which this study intended to analyze.

When blinds are applied to the double pane window as shown in Fig. 3, the equation of thermal equilibrium between glasses and blinds is added, along with the equation of thermal equilibrium between glasses. Equation (3) is the equation of thermal equilibrium on the glass surface (Glass layer #2), where $1 - \rho_4 \rho_{sh}$ indicates the exchange of longwave radiation between glasses and blinds due to inter-reflection. The convective heat transfer from the glass surface to the air layer can be expressed as $q_{c,gl} = h_{cv}(\theta_4 - T_{gap})$ where $T_{gap}$ indicates the temperature of air layer (K) and $h_{cv}$ indicates the convective heat transfer coefficient ($\mathrm{W \cdot m^{-2} \cdot K^{-1}}$). On the contrary, the convective heat transfer on the blind layer can be expressed as $q_{c,gl} = h_{cv}(\theta_5 - T_{gap})$ by the blind surface temperature, and $h_{cv} = 2h_v + 4v$ is used as the effective convective heat transfer coefficient on the air layer. The convective heat transfer coefficient corresponding to the stagnant air layer is applied for $h_c$, and $v$ shows air flow (m/s), so the variation of coefficients according to the air flow can be expected [6,13].

## 3 Simulation Model and Condition

### 3.1 Simulation Model

The simulation model used in this study is a virtual three-story office building where venetian blinds are installed, and this building is 49 m long, 33 m wide with the story height of 3 m which is divided into the top, middle and ground floors. The 49 m-long sides faced south and north, respectively; and the 33 m-long sides faced east and west, respectively (Fig. 4). An analysis was carried out in each perimeter zone (east, west, south and north) in the middle floor. The standard weather data of Seoul area provided by the Korean Solar Energy Society was used as the weather data for the analysis [8]. The standard weather data of Seoul city used in this study are TRY (Test Reference Year) format based on ISO (International Standard Organization) 15972-4. The three candidate "best typical years" are first selected based on outdoor dry-bulb temperature, horizontal solar radiation and relative humidity. And then, the "best typical year" is finally selected based on the outdoor air velocity data. In case of Seoul weather data

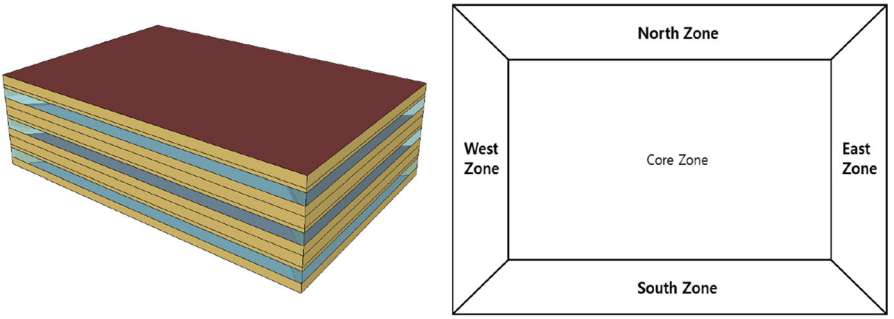


**Fig. 4** Simulated building model: (a) building model; (b) interior and exterior zone [14]

**Table 2** Properties of building construction [14]

| | Materials | Thickness (m) | Conductivity ($W \cdot m^{-1} \cdot K^{-1}$) |
|---|---|---|---|
| Ext wall | M15 200 mm heavyweight concrete | 0.2032 | 1.95 |
| | I02 70 mm insulation board | 0.07 | 0.034 |
| | F04 Wall air space resistance | – | 0.15 |
| | G01a 19 mm gypsum board | 0.019 | 0.16 |
| Roof | M11 100 mm lightweight concrete | 0.1016 | 0.53 |
| | I02 150 mm insulation board | 0.15 | 0.034 |
| | F16 Acoustic tile | 0.0191 | 0.06 |
| Groud floor | M15 200 mm heavyweight concrete | 0.2032 | 1.95 |
| | I02 70 mm insulation board | 0.07 | 0.034 |
| | M15 200 mm heavyweight concrete | 0.2032 | 1.95 |
| Ceiling | M11 100 mm lightweight concrete | 0.1016 | 0.53 |
| | F05 ceiling air space resistance | – | 0.18 |
| | F16 acoustic tile | 0.0191 | 0.06 |

provided by the Korean Solar Energy Society, the standard weather data are produced from the statistical analysis of 20 year weather data from 1986 to 2005 [15].

Table 2 shows the major skin element components and properties of each simulation model. The double pane glass (6 mm Clear + 12 mm Air + 6 mm Clear) was applied for the window as shown in Fig. 5 and it has optical and material characteristics of SHGC 0.765, Tvis 0.812, U-value 2.724 $W \cdot m^{-2} \cdot K^{-1}$. The blinds applied to analyze a change in the heat gain through window and develop an optimal control algorithm are venetian internal blinds, of which reflectance is 0.9, heat conductivity is 0.9 $W \cdot m^{-1} \cdot K$ and emissivity is 0.9. In addition, the width of a slat is 0.048 m, the spacing between slats is 0.048 m and the spacing between glass and blind is 0.05 m. Other detailed items are shown in Table 3. The range of slat angle for optimal control is between 0° and 90°": 0° indicates full close and 90 ° indicates full open.

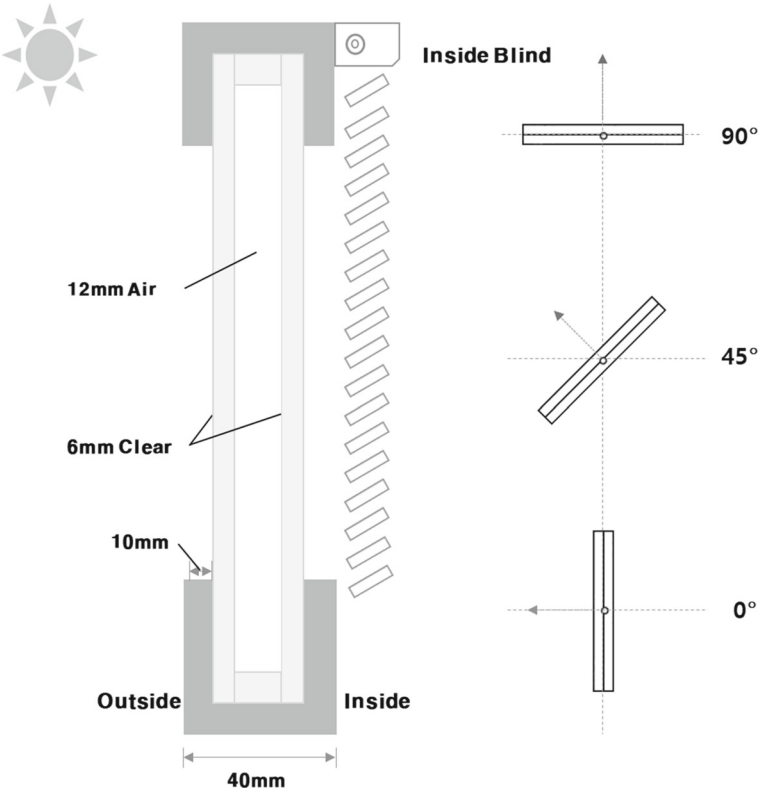


**Fig. 5** Configuration of blind slat and slat angle

**Table 3** Properties of blind slat [6,14]

| Field | Unit | Value |
|---|---|---|
| Blind position | | Inside blind |
| Slat width | m | 0.048 |
| Slat separation | m | 0.048 |
| Slat thickness | m | 0.002 |
| Blind to glass distance | m | 0.050 |
| Slat reflectance | % | 90 |
| Slat infrared hemispherical emissivity | – | 0.900 |
| Slat conductivity | $W \cdot m^{-1} \cdot K^{-1}$ | 0.900 |
| Slat angle | ° | 0–90 |

$17 m^2$/person for occupancy, $10.8 W/m^2$ for lighting load and $8.6 W/m^2$ for equipment load were set, respectively, for internal heat gain applied to the simulation as shown in Table 4, and the consequent internal heat gain schedule is as shown in Fig. 6. 21 °C at the time of heating and 26 °C at the time of cooling were set as each indoor

**Table 4** Internal heat gain [6]

| | Value | Radiant fraction |
|---|---|---|
| Occupancy | 17 $m^2$/person | 0.6 |
| Lighting loads | 10.8 $W/m^2$ | 0.32 |
| Equipment loads | 8.6 $W/m^2$ | 0.4 |

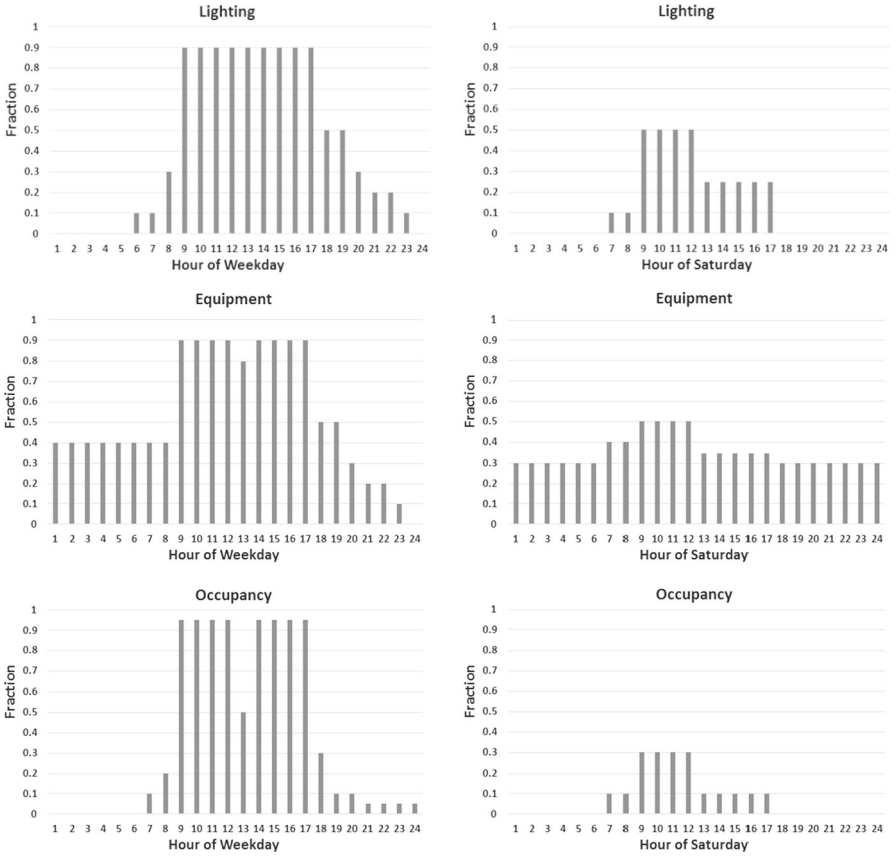


**Fig. 6** Internal heat gain schedule

temperature, and a different heat gain schedule was set for weekdays and Saturday. The simulation was carried out on the assumption of no air-conditioning on Sunday in a virtual office building.

As a final step of the development of the simulation model to be used in the study, the validation process is briefly carried out to ensure that the model can properly predict the thermal load and blind performance. Oh et al.'s data were used for the validation process in this study, since this study provides both conditions and results in relative detail [1,6]. Similar conditions of internal heat gain, blind properties and building constructions are used between Oh's study and this study. In addition, the

orientation of the zone, which is the target zone for the validation, is south in both studies. The heating and cooling load in Oh's study showed 12.3 and 67.2 $kWh/m^2$, respectively, without blind installation. The current model in this study showed 10.3 and 65.5 $kWh/m^2$ [14], respectively, under the same conditions. The discrepancies are due to different weather conditions and slightly different window-to-wall ratio and building construction considered in those two studies. However, two data sets are in good agreement and thus the new model properly predicts the thermal load and blind performance.

### 3.2 Simulation Condition

In this study, the analysis was carried out separately for the cooling period (June, July and August) and the heating period (January, February and December) in order to develop an optimal venetian blind control algorithm and analyze its building energy saving performance in case of applying it. IdealLoadsAirSystem Object on EnergyPlus, which was the air-conditioning method excluding the efficiency of the HVAC system and plant, was used in order to analyze data of cooling, heating and lighting load generated inside the simulation model. At this time, 21 °C from 07:00 to 18:00 for heating and 26 °C from 07:00 to 19:00 for cooling were set as the indoor set temperatures of the air-conditioning system. The simulation was carried out under 12 conditions in order to develop the control algorithm for all orientations with the window-to-wall ratio of 33 %, 50 % and 70 %, respectively, as shown in Table 5.

Continuous lighting control, in which lighting energy decreased linearly as the amount of natural lighting that varied according to the window-to-wall ratio, orientation and blind slat angle increased, was applied for the lighting control in this study. In addition, 500 lux that fell between 300 lux, the minimum recommended levels of illumination for office, and 600 lux, the maximum recommended levels of illumination

**Table 5** Simulation cases [16]

| Case | WWR (window-to-wall ratio) (%) | Window orientation |
|---|---|---|
| East_33 % | 33 | East |
| West_33 % | | West |
| South_33 % | | South |
| North_33 % | | North |
| East_50 % | 50 | East |
| West_50 % | | West |
| South_50 % | | South |
| North_50 % | | North |
| East_70 % | 70 | East |
| West_70 % | | West |
| South_70 % | | South |
| North_70 % | | North |

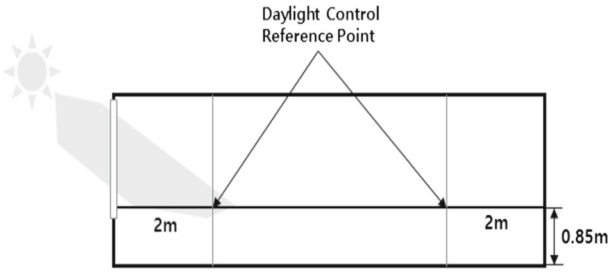


**Fig. 7** Lighting control sensor position of simulation model [6,11]

for office, according to the Korean Industrial Standard, was set as the recommended levels of illumination for indoor lighting control. The detection sensor was set at 2 m away from the window as shown in Fig. 7 so that only 20 % of lighting energy was operated when the indoor illumination intensity was 500 lux or higher [6].

## 4 Development of Optimal Control Algorithm

### 4.1 Necessity and Development Process of Optimal Control Algorithm

In this study, the optimal blind control algorithm was developed through the process, as shown in Fig. 8, based on previous studies [6] in which the development method of optimal control algorithm was established. The surface solar radiation, which were considered enough to be a variable condition for natural lighting and the indoor heat

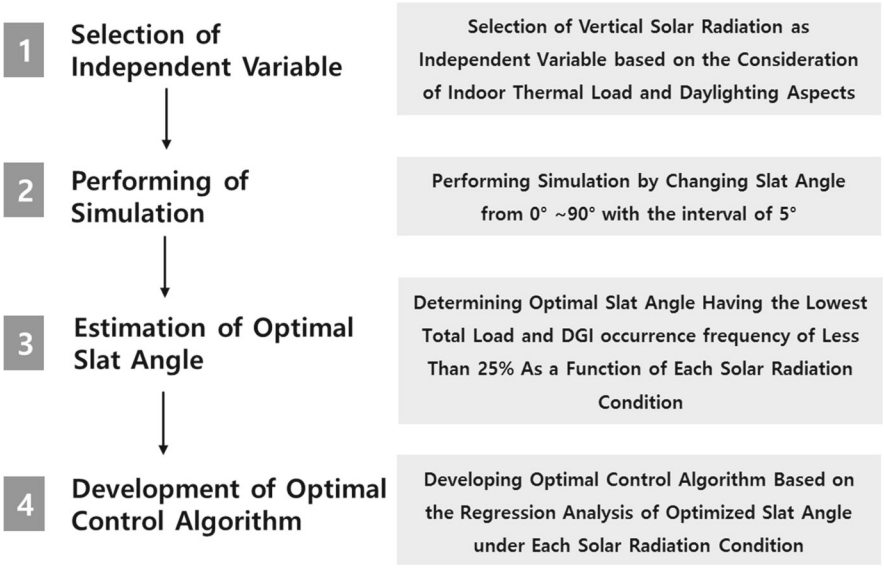


**Fig. 8** Process of optimal slat angle control algorithm development [16]

gain, were selected as input variables for developing control algorithms [6,16]. Then, the blind slat angle in the range between 0° and 90° was divided by 5° and the simulation was carried out. Based on the simulation result for each slat angle, data of cooling, heating and lighting loads for each surface solar radiation section were collected. At this time, the surface solar radiation section was $100\,W \cdot m^{-2}$. The angle with the lowest total indoor load (cooling + heating + lighting) among data with less than 25 % for the occurrence frequency of discomfort glare index was selected for the optimized slat angle for each section. After that, the optimal control algorithm was developed based on the optimal angle by surface solar radiation section through the regression analysis [6,14]. Based on such method, a different control algorithm for each window-to-wall ratio and orientation was developed after applying such method to the 33 %, 50 % and 70 % analysis models equally. Figures 9 and 10 show the graphs indicating total energy and the occurrence frequency of discomfort glare index by slat angle according to surface solar radiation, which was the input variable, for the cooling period and the heating period, and the analysis was carried out based on the representative condition of East_50 %. Since the surface solar radiation is an external condition that does not change according to the slat angle which is an analysis variable and thus, the number of data drawn from each slat angle is the same and figures vary, the total energy consumption and occurrence frequency of discomfort glare index can be compared and analyzed [17].

Figure 9 is the graph showing the selection of optimized slat angle according to surface solar radiation by section in the cooling period (June, July and August). The lowest total building energy consumption was measured when the surface solar radiation was $100\,W \cdot m^{-2}$ and the slat angle was 40° that was the condition of partial open. In case of 90° which is the full open of slat, it is advantageous for lighting energy as the inflow of solar radiation increases, but it is disadvantageous for cooling energy. In case of 0° which is the full close of slat, it is advantageous for cooling energy but it is disadvantageous for heating energy. It was judged that 40° was the optimized slat angle in the correlation between the lighting energy consumption and cooling energy consumption. In addition, as the surface solar radiation increases gradually, the slat angle becomes closer to 0°. This can be interpreted that the amount of lighting energy consumption increase is larger than the amount of cooling energy consumption decrease due to the blocking of inflow of solar radiation.

Figure 10 is the graph showing the selection of optimized slat angle according to surface solar radiation by section in the heating period (January, February, December), and unlike the cooling period, the surface solar radiation was less than $600\,W \cdot m^{-2}$. The lowest total building energy consumption was measured when the surface solar radiation was less than $100\,W \cdot m^{-2}$ and the slat angle was 90° which was the condition of full open. As the slat was fully open, the inflow of solar radiation increased, reducing heating and lighting energy consumption. After that, as the surface solar radiation increases, the occurrence frequency of discomfort glare index increases. This results from increased incidence angle of solar radiation in the heating period rather than the cooling period. In addition, in the heating period, as the slat angle increases, the building energy consumption decreases regardless of the surface solar radiation; and in consideration of the occurrence frequency of discomfort glare index, a slat angle which does not exceed it becomes the optimal position. After that, the optimal slat

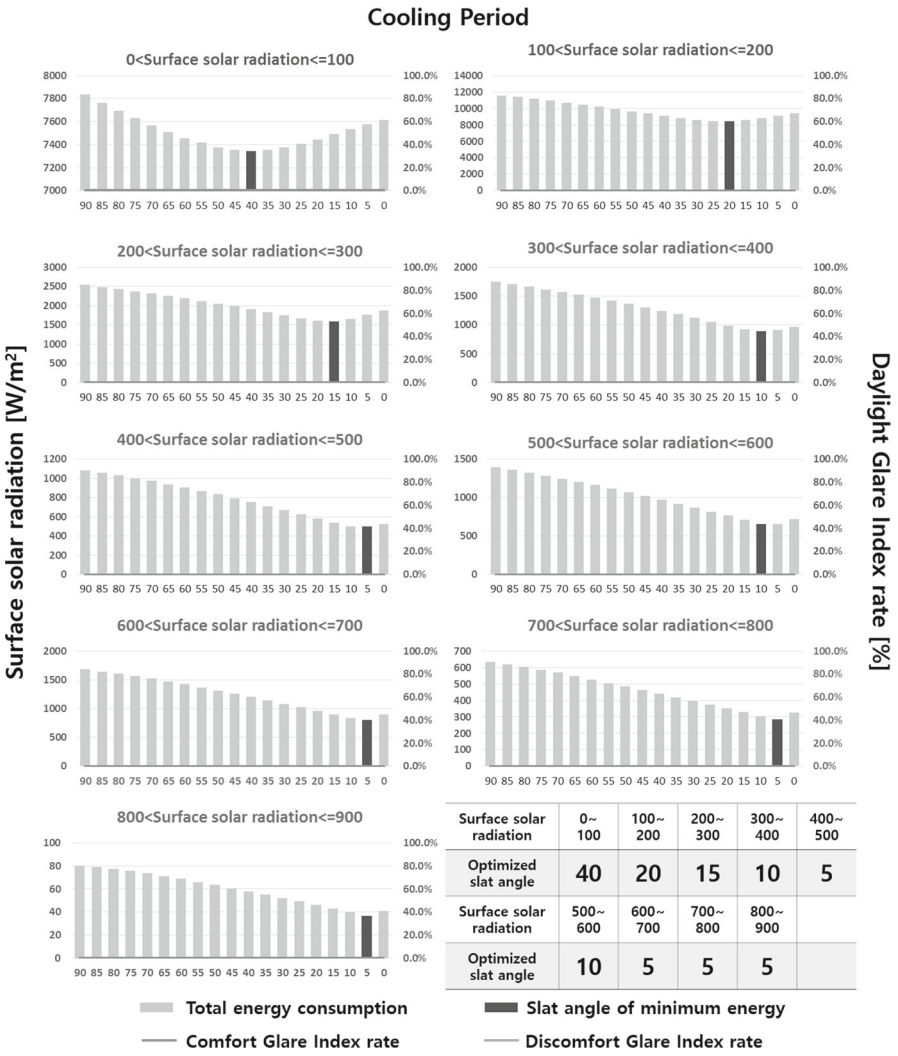


**Fig. 9** Selection of optimized slat angle according to surface solar radiation in cooling period

angle algorithm for the cooling and heating periods in all conditions was developed according to such methods [17].

## 4.2 Optimal Control Algorithm for the Cooling and Heating Periods

Tables 6 and 7 show the optimized slat angle of blinds in the cooling period (June, July, August) and heating period (January, February, December) developed according to the surface solar radiation, after the simulation was carried out based on each optimal control algorithm development method. The developed optimized angle varied

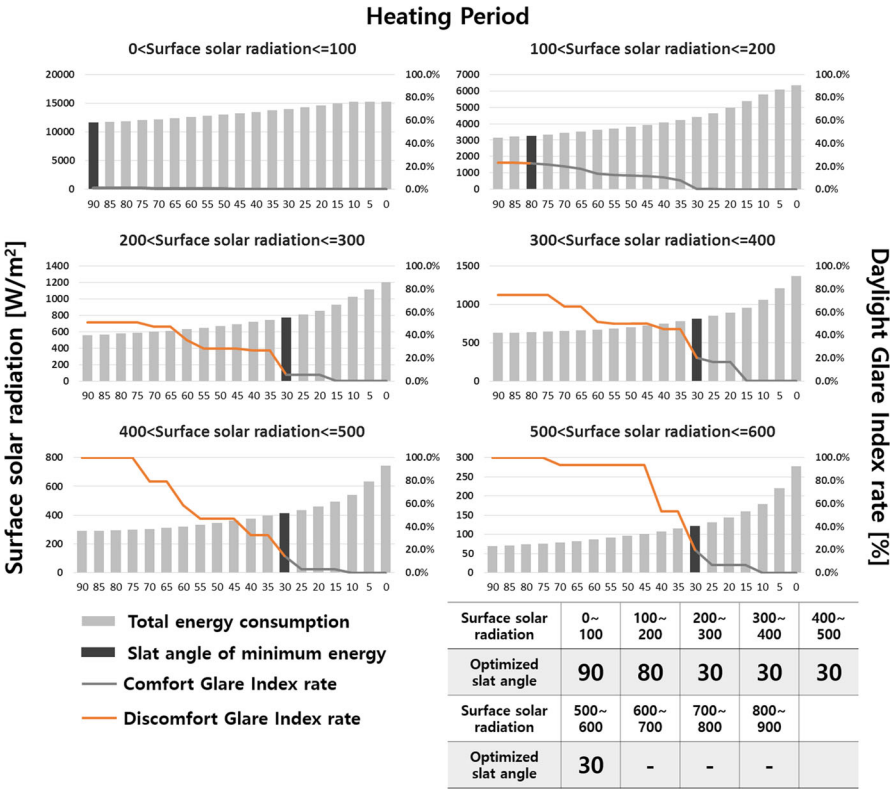


| Surface solar radiation | 0~100 | 100~200 | 200~300 | 300~400 | 400~500 |
|---|---|---|---|---|---|
| Optimized slat angle | 90 | 80 | 30 | 30 | 30 |
| Surface solar radiation | 500~600 | 600~700 | 700~800 | 800~900 | |
| Optimized slat angle | 30 | - | - | - | |

**Fig. 10** Selection of optimized slat angle according to surface solar radiation in heating period

depending on the window-to-wall ratio even for the same orientation, and it also varied depending on the orientation even for the same window-to-wall ratio. In addition, the surface solar radiation measured in the cooling period ranged from $0\,W \cdot m^{-2}$ to $900\,W \cdot m^{-2}$ for east and west, from $0\,W \cdot m^{-2}$ to $600\,W \cdot m^{-2}$ for south and from $0\,W \cdot m^{-2}$ to $300\,W \cdot m^{-2}$ for north, whereas it ranged from $0\,W \cdot m^{-2}$ to $600\,W \cdot m^{-2}$ for east, from $0\,W \cdot m^{-2}$ to $700\,W \cdot m^{-2}$ for west, from $0\,W \cdot m^{-2}$ to $900\,W \cdot m^{-2}$ for south and from $0\,W \cdot m^{-2}$ to $200\,W \cdot m^{-2}$ for north in the heating period. In the case of south, the surface solar radiation was less than $600\,W \cdot m^{-2}$ in the cooling period due to a high incidence angle of solar radiation, but it was less than $900\,W \cdot m^{-2}$ in the heating period due to a low incidence angle of solar radiation. Especially, in the case of north, a lower surface solar radiation is shown in the cooling period as well as the heating period in comparison with other orientations, and this is because only the diffused solar radiation is brought into the indoors through the window without the effects of direct solar radiation.

The optimal control algorithm can be developed from the relationship between the surface solar radiation shown in Tables 6 and 7 and the optimized angle for each condition; and it can be defined as shown in Eq. (3). In the equation, x indicates the surface solar radiation, and each coefficient indicates the constant value calculated

**Table 6** Optimized slat angle in cooling period

| Surface solar radiation ($W \cdot m^{-2}$) | East | | | West | | | South | | | North | | |
|---|---|---|---|---|---|---|---|---|---|---|---|---|
| | 33 % | 50 % | 70 % | 33 % | 50 % | 70 % | 33 % | 50 % | 70 % | 33 % | 50 % | 70 % |
| 0–100 | 50 | 40 | 30 | 60 | 45 | 35 | 60 | 40 | 30 | 70 | 50 | 35 |
| 100–200 | 35 | 20 | 15 | 40 | 25 | 20 | 40 | 25 | 20 | 40 | 25 | 10 |
| 200–300 | 25 | 15 | 10 | 25 | 15 | 10 | 25 | 15 | 15 | 25 | 15 | 10 |
| 300–400 | 15 | 10 | 5 | 15 | 10 | 10 | 20 | 15 | 10 | | | |
| 400–500 | 10 | 5 | 5 | 10 | 5 | 5 | 15 | 10 | 10 | | | |
| 500–600 | 10 | 10 | 5 | 10 | 5 | 0 | 0 | 0 | 0 | | | |
| 600–700 | 10 | 5 | 5 | 0 | 5 | 0 | | | | | | |
| 700–800 | 10 | 5 | 5 | 0 | 0 | 0 | | | | | | |
| 800–900 | 10 | 5 | 5 | 5 | 5 | 0 | | | | | | |

**Table 7** Optimized slat angle in heating period

| Surface solar radiation ($W \cdot m^{-2}$) | East | | | West | | | South | | | North | | |
|---|---|---|---|---|---|---|---|---|---|---|---|---|
| | 33 % | 50 % | 70 % | 33 % | 50 % | 70 % | 33 % | 50 % | 70 % | 33 % | 50 % | 70 % |
| 0–100 | 90 | 90 | 90 | 90 | 90 | 90 | 90 | 90 | 90 | 90 | 90 | 90 |
| 100–200 | 90 | 75 | 70 | 90 | 85 | 70 | 40 | 35 | 35 | 90 | 90 | 90 |
| 200–300 | 40 | 30 | 35 | 35 | 35 | 35 | 35 | 35 | 35 | | | |
| 300–400 | 30 | 30 | 30 | 30 | 30 | 30 | 50 | 40 | 35 | | | |
| 400–500 | 30 | 30 | 25 | 30 | 30 | 30 | 45 | 40 | 25 | | | |
| 500–600 | 30 | 30 | 25 | 30 | 30 | 30 | 35 | 25 | 15 | | | |
| 600–700 | | | | 25 | 25 | 25 | 30 | 20 | 10 | | | |
| 700–800 | | | | | | | 25 | 15 | 10 | | | |
| 800–900 | | | | | | | 20 | 10 | 5 | | | |

through the regression analysis. x is limited the same as the range of surface solar radiation by condition in the developed equation.

$$\text{Optimized Slat Angle}_{(\textbf{\textit{Orientation}}, Window-wall-ratio)} = Ax^4 + \mathrm{B}x^3 + Cx^2 + Dx + E \tag{3}$$

Figure 11 shows the graphs indicating the optimized slat angle control algorithm by the section of solar radiation according to window-to-wall ratio change for each orientation during summer and winter. At first, in case of south in the cooling period, the blind slat angle increases gradually as the surface solar radiation increases; and the pattern of more closed slat angle is also shown in the condition of 70 % for the window-to-wall ratio than the condition of 33 % for the window-to-wall ratio. It is judged that this is to respond to a subsequent increase in the indoor cooling load as the window-to-wall ratio increased. In the case of west, a similar pattern with the east is

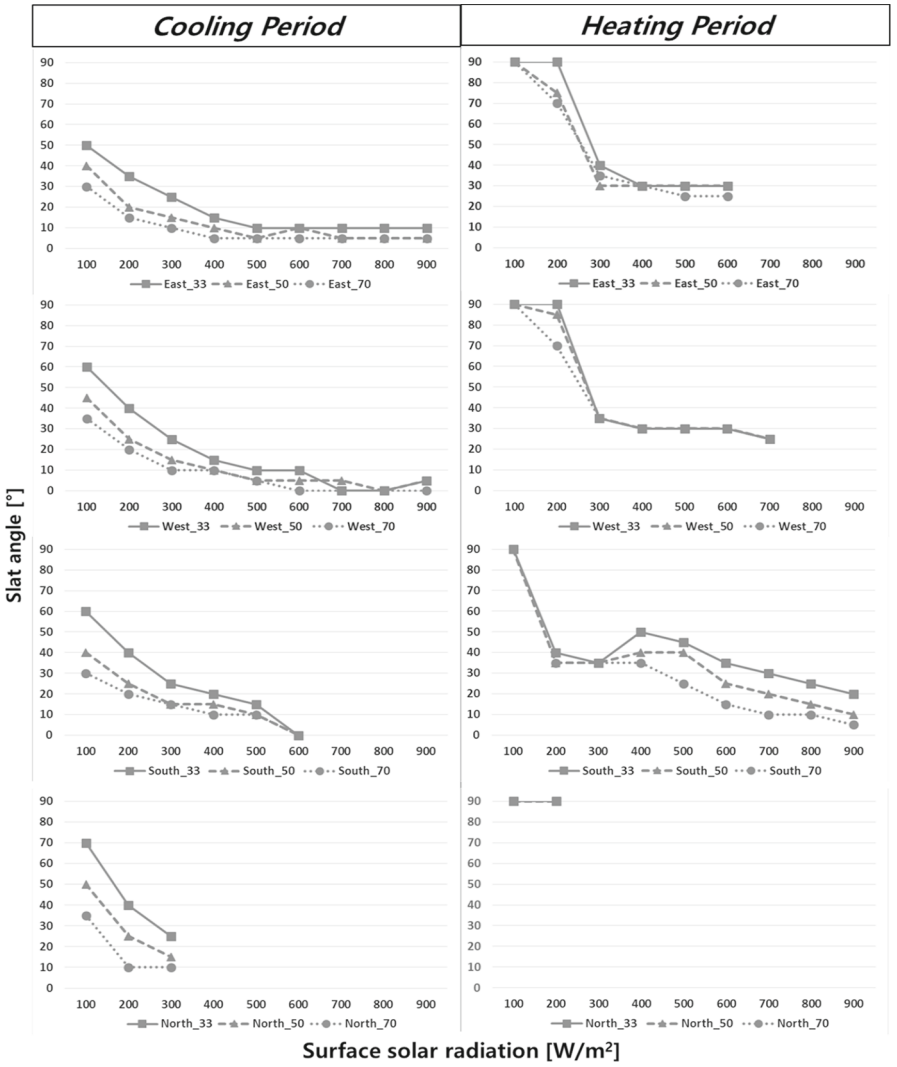


**Fig. 11** Optimized slat angle control algorithm

shown, but a slat angle larger than the slat angle in the east is shown at the section with a low surface solar radiation of 200 $W \cdot m^{-2}$. As the surface solar radiation increases, a similar pattern of slat angle with east is shown. In the case of south, as the surface solar radiation increased, the slat angle increased gradually; and the slat angle was 0° in the section between 500 $W \cdot m^{-2}$ and 600 $W \cdot m^{-2}$, showing full close. In the case of north, the surface solar radiation was 300 $W \cdot m^{-2}$, and a clear difference in the slat angle over 15° for each surface solar radiation section was shown according to a change in the window-to-wall ratio.

In the case of east in heating period, the surface solar radiation was $200\,\mathrm{W}\cdot\mathrm{m}^{-2}$ and the slat angle was over 70° unlike the cooling period, showing a pattern of opening the slat slightly. After that, as the surface solar radiation increased, a pattern of closing the slat slightly is shown, and this is to prevent a discomfort glare that occurs due to an incidence angle of solar radiation in the heating period. A similar pattern is also shown in west, and the same slat angle is shown regardless of window-to-wall ratio in the section of surface solar radiation over $300\,\mathrm{W}\cdot\mathrm{m}^{-2}$. In the case of south, a similar pattern is shown in the section less than $300\,\mathrm{W}\cdot\mathrm{m}^{-2}$ regardless of the window-to-wall ratio, but in the section over $300\,\mathrm{W}\cdot\mathrm{m}^{-2}$, as the window-to-wall ratio increases, the slat is more closed. This results from an increase in the occurrence frequency of discomfort glare index as the window-to-wall ratio increased due to a high incidence angle of solar radiation in the heating period in south. Lastly, in the case of north, the same optimal control algorithm was developed in all conditions in all surface solar radiation sections regardless of the window-to-wall ratio. No cooling energy was consumed in the heating period and no discomfort glare occurred, so the slat was fully open to increase the inflow of solar radiation, resulting in the reduction in heating and cooling load.

## 5 Energy Performance

### 5.1 Analysis of Energy on the Representative Day

By selecting East_50 % as the representative condition and applying to the analysis model the optimized slat angle calculated as shown above, the following three changes were analyzed: a change in the optimized slat angle according to the surface solar radiation by hour, a change in cooling and heating energy according to slat angle change, and a change in lighting energy for the level of illumination. Figure 12 shows the result of representative days for cooling (August 8 and 9) and Fig. 13 indicates the result of representative days for heating (January 24 and 25), showing graphs comparing with the fixed slat condition in which the slat angle is fixed at 45°.

At first, according to the result of representative days for cooling (August 8 and 9), the slat angle is maintained at 45° for the fixing type slat condition, but the slat angle is controlled according to the surface solar radiation under the condition where the optimized slat angle produced above is applied. As shown in the analysis result above, as the surface solar radiation is larger, the slat angle is controlled closely to 0° which is full close, indicating that it is controlled properly according to the surface solar radiation. In the case of heating energy in the cooling period, there is no significant difference between the fixed slat condition and the optimized slat condition, and the heating energy consumption is also less.

When analyzing the cooling energy, both fixed slat condition and the optimized slat condition show the pattern where cooling energy consumption increases as the surface solar radiation increases. However, the cooling energy consumption in the optimized slat condition is lower than the cooling energy consumption under the fixed slat condition, and the cooling energy consumption at the highest surface solar radiation is up to approximately 40 % lesser than the cooling energy consumption under

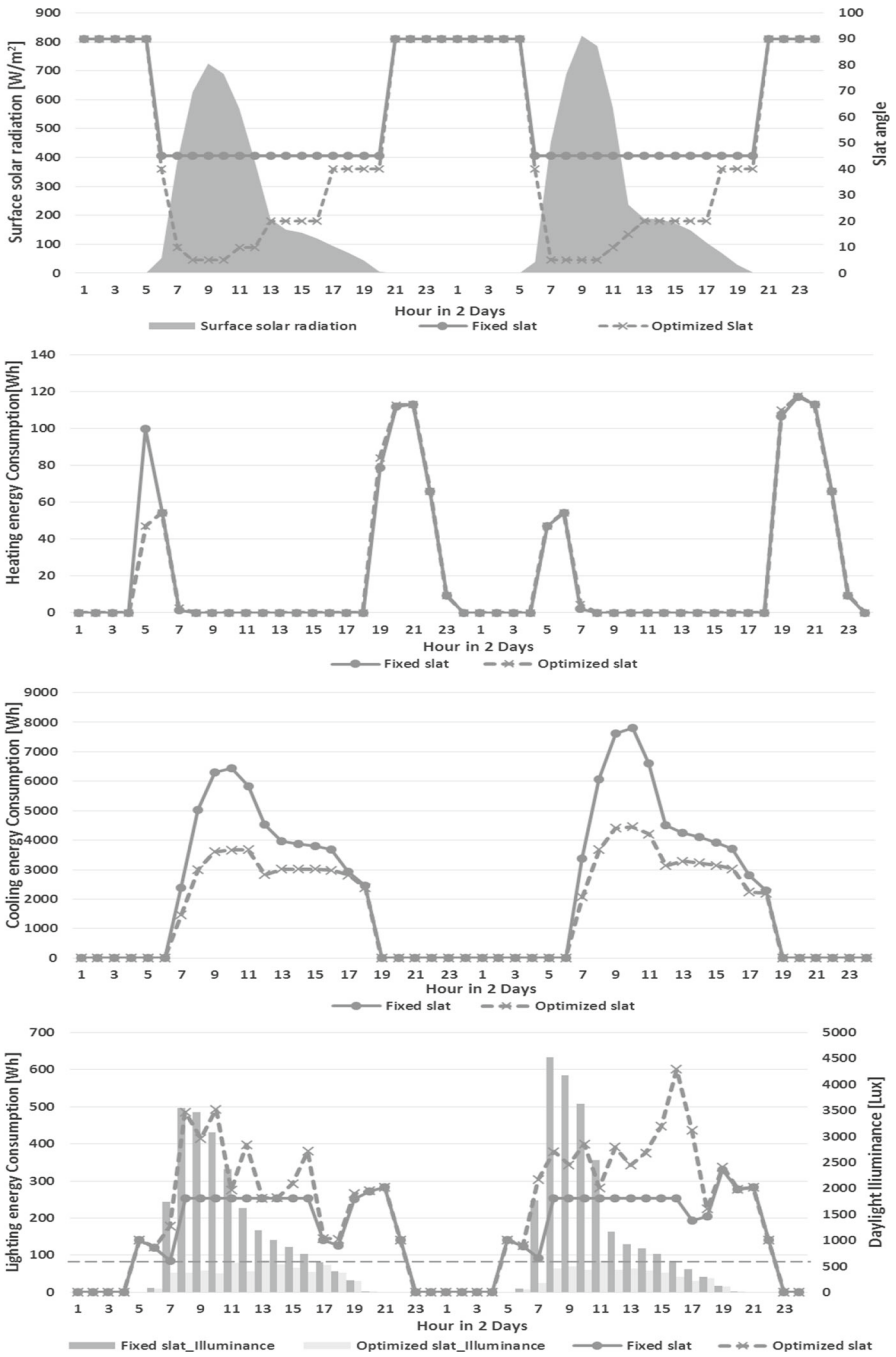


**Fig. 12** Surface solar radiation and optimized slat angle (1st), heating energy (2nd), cooling energy (3rd), daylight illuminance and lighting energy (4th) in cooling period representative days (August 8, 9)

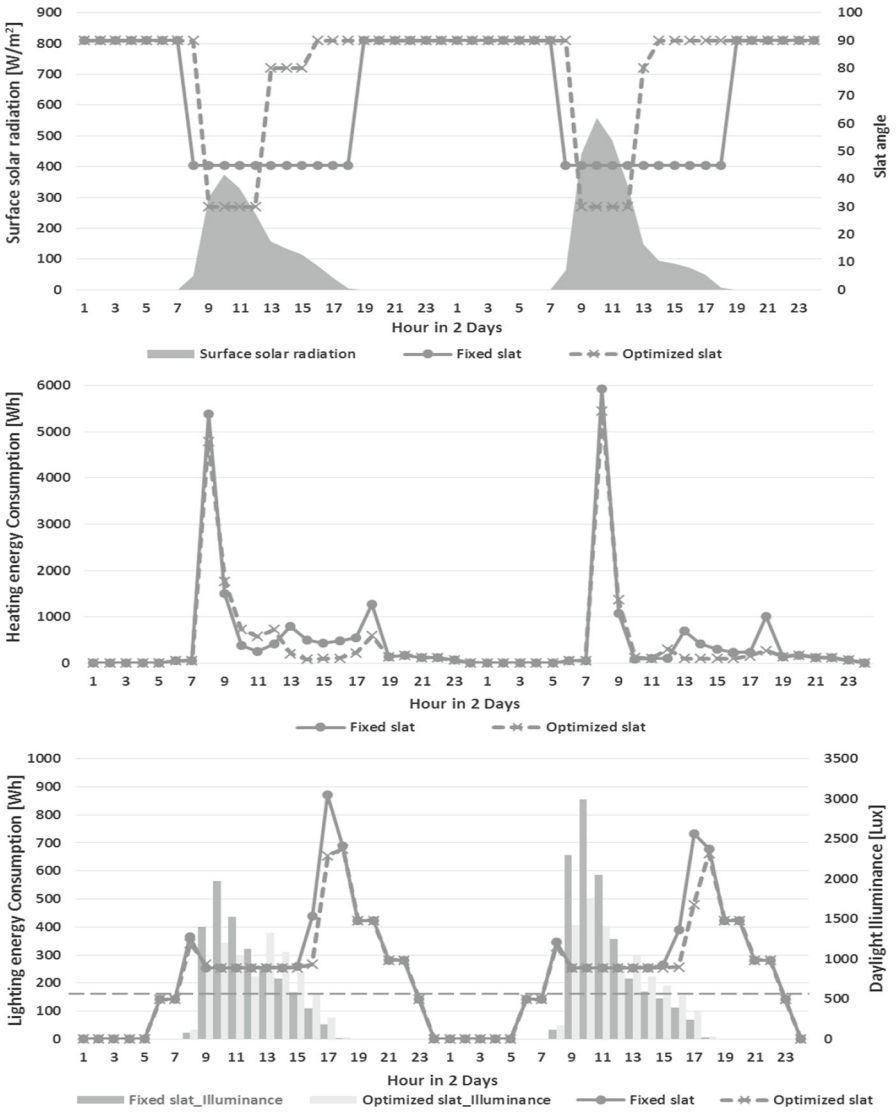


**Fig. 13** Surface solar radiation and optimized slat angle (1st), heating energy (2nd), daylight illuminance and lighting energy (3rd) in heating period representative days (January 24, 25)

the fixed slat condition. In addition, as the surface solar radiation is higher, a difference in cooling energy between two conditions becomes larger. This may result from the fact that as the surface solar radiation decreases, the slat angle in the optimized slat condition becomes closer to 45° which is the slat angle under the fixed slat condition.

The lighting energy consumption changes according to the level of illumination of detection sensor, and the level of illumination in the fixed slat condition shows a similar pattern with the surface solar radiation. In addition, when the level of illumination

exceeds 500 lux due to natural lighting, a fixed level of illumination is shown according to the lighting schedule. However, in the case of the optimized slat condition, an angle is often smaller than 45°, so the level of illumination due to natural lighting (excluding the level of illumination due to indoor lighting) measures less than 500 lux. Subsequently, the lighting energy consumption becomes higher in comparison with the fixed slat condition in order to meet 500 lux as the minimum indoor illumination intensity. However, a difference in the lighting energy consumption between two conditions is smaller in comparison with cooling energy consumption. It can be seen from the cooling energy and lighting energy graphs that when controlling the optimized slat angle, a decrease in the cooling energy consumption is larger than an increase in the lighting energy that occurs due to the closing of slat according to an increase in the surface solar radiation.

When analyzing the result of representative days for heating (January 24 and 25) in Fig. 13, the slat angle is controlled according to the surface solar radiation as with the representative days for cooling.

In comparison with the cooling period, the optimized slat angle in the heating period shows a pattern where the slat is almost fully open at less than a certain level of surface solar radiation. This results from a decrease in heating energy and lighting energy consumption as the slat is open wider in the range where no discomfort glare occurs, as with the analysis result of optimized slat angle in the heating period above. It can be judged that proper operation through the control of the slat angle is carried out as shown in the above analysis result indicating that a discomfort glare occurs at a certain level of surface solar radiation or higher, so the slat angle is decreased in order to prevent it.

When analyzing the heating energy, a difference in the consumption of heating energy occurred according to the slat opening status in the comparison between the fixed slat condition and the optimized slat condition. As the result of analysis carried out previously, the heating energy changed according to the slat angle; and as the slat was open closely to 90°, the inflow of solar radiation increased and the consumption of heating energy decreased accordingly. In the case of cooling energy, it was not measured in the heating period, and in the case of lighting energy, its consumption changed according to the level of illumination and lighting schedule as with the cooling period. However, although the optimized slat angle was controlled at 30° during the day time of heating period unlike the cooling period, the level of illumination due to natural lighting was 500 lux or higher, indicating that there was no significant change in the lighting energy consumption. However, the level of illumination on the fixed slat condition in the range of less surface solar radiation became smaller than the level of illumination due to open slat angle on the optimized slat condition, indicating that the lighting energy consumption increased.

### 5.2 Annual Energy Performance According to Window-to-Wall Ratio and Orientation

Figure 14 shows the building energy consumption according to the window-to-wall ratio for each orientation under the fixed slat condition where the slat angle in the cool-

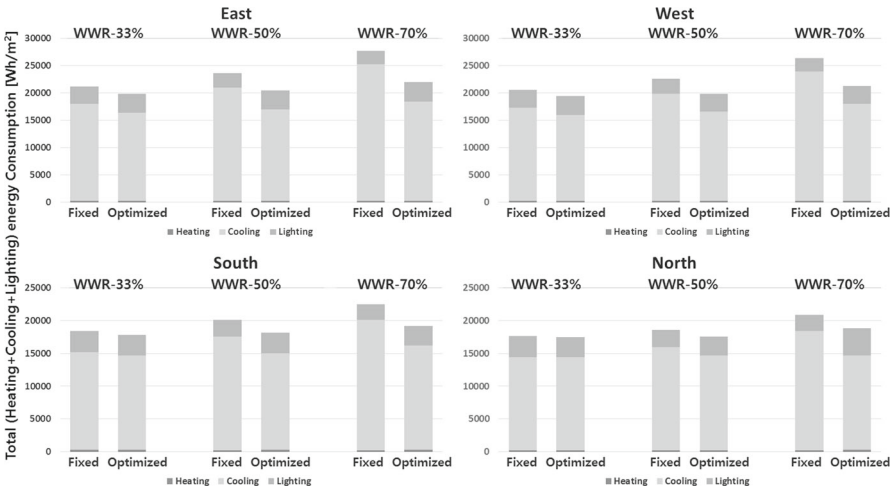


**Fig. 14** Building energy consumption according to orientation and window-to-wall ratio in cooling period compared with fixed slat angle

ing period is fixed at 45° and under the optimized slat condition where the optimized slat angle according to the surface solar radiation is applied. In addition, Table 8 shows the energy consumption data responding to each condition and the amount of energy consumption reduction in the optimized slat condition. At first, this shows that as the window-to-wall ratio increased in all orientations, the amount of building energy consumption reduction also increased. In the east, a 6.24 % saving in East_33 % condition and a 20.73 % saving in East_70 % condition were shown. In the west, a 5.85 % saving in West_33 % condition and a 19.4 % saving in West_70 % condition were shown, and in the south, a 3.22 % saving in South_33 % condition and a 14.98 % saving in South_70 % condition were shown. In the north, there was no significant difference in the building energy consumption between the fixed slat condition and the optimized slat condition in the condition of 33 % for the window-to-wall ratio, but a 9.59 % building energy saving was shown in the condition of 70 % for the window-to-wall ratio. Likewise, as the window-to-wall ratio increases, the building energy saving rate also increases, and this is because as the window-to-wall ratio increases, the amount of solar radiation brought into the building increases and the effects of blind slat angle also increase accordingly.

Figure 15 and Table 9 show the building energy consumption data (cooling + heating + lighting) in the fixed slat condition that fixed the slat angle at 45° when the optimized slat in heating period was applied the same as the previous result. In the heating period, the window-to-wall ratio increased for each orientation, the saving rate also increased as in the cooling period, and approximately 10 % saving rate was shown in most conditions. However, the building energy saving rate for each condition that increased as the window-to-wall ratio increased was lower than that in the cooling period. This is probably due to the following facts: that the opening of slat in the heating period resulted in heating energy and lighting energy saving, and that due to a high incident angle of solar radiation penetrated through the window, the occurrence frequency of

**Table 8** Energy consumption (kWh · $m^{-2}$) and reduction rate (%) by orientation and WWR in cooling period

| Orientation | East | | | West | | | South | | | North | | |
|---|---|---|---|---|---|---|---|---|---|---|---|---|
| WWR | 33 % | 50 % | 70 % | 33 % | 50 % | 70 % | 33 % | 50 % | 70 % | 33 % | 50 % | 70 % |
| Fixed slat total energy consumption | 21.2 | 23.6 | 27.7 | 20.6 | 22.6 | 26.4 | 18.4 | 20.1 | 22.5 | 17.6 | 18.6 | 20.8 |
| Optimized slat total energy consumption | 19.8 | 20.5 | 21.9 | 19.4 | 19.9 | 21.3 | 17.8 | 18.1 | 19.1 | 17.4 | 17.5 | 18.8 |
| Reduction rate (%) | 6.24 | 13.08 | 20.73 | 5.85 | 11.94 | 19.4 | 3.22 | 9.91 | 14.98 | 0.98 | 5.34 | 9.59 |

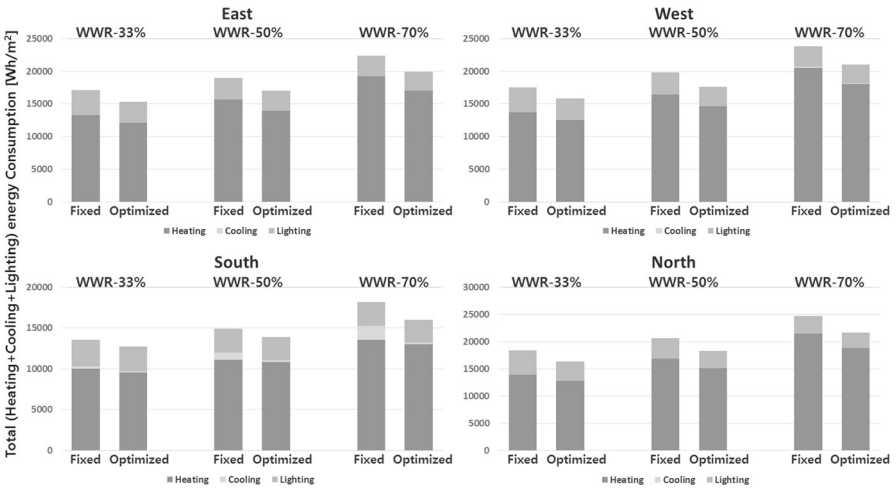


**Fig. 15** Building energy consumption according to orientation and window-to-wall ratio in heating period compared with fixed slat angle

discomfort glare index more increased in comparison with the cooling period, and that to prevent this, the slat was not fully open at the time of high surface solar radiation and a slat angle which was close to 0° was applied.

## 6 Conclusion

In this study, optimized slat angle control algorithms for venetian blinds according to a change in the window-to-wall ratio and orientation was developed separately for the cooling period and the heating period in order to consider various variables comprehensively for controlling the blinds. The developed algorithms varied according to the orientation, window-to-wall ratio, cooling period and heating period; and the comparative analysis of building energy performance for each condition was carried out by applying the developed algorithms to the simulations. The conclusions of this study are as follows.

- As a result of developing an optimized slat angle algorithm for each condition, a different algorithm for each window-to-wall ratio and orientation considered in this study was developed.
- For the same orientation, the algorithms developed in the cooling period and the heating period show a pattern where the same or more closing slat angle of the blinds is shown as the window-to-wall ratio increases.
- For the same window-to-wall ratio in the cooling period, the optimized slat angle in west is larger than the optimized slat angle in east at the section where the surface solar radiation is less than 200 $W \cdot m^{-2}$.
- When applying the optimized slat angle in the cooling period, a decrease in the cooling energy consumption is larger than an increase in the lighting energy that

**Table 9** Energy consumption (kWh · $m^{-2}$) and reduction rate (%) by orientation and WWR in heating period

| Orientation | East | | | West | | | South | | | North | | |
|---|---|---|---|---|---|---|---|---|---|---|---|---|
| WWR | 33 % | 50 % | 70 % | 33 % | 50 % | 70 % | 33 % | 50 % | 70 % | 33 % | 50 % | 70 % |
| Fixed slat total energy consumption | 17.1 | 19.0 | 22.4 | 17.5 | 19.8 | 23.8 | 13.5 | 14.9 | 18.2 | 18.4 | 20.6 | 24.7 |
| Optimized slat total energy consumption | 15.3 | 17.0 | 19.9 | 15.8 | 17.6 | 21.0 | 12.7 | 13.9 | 15.9 | 16.3 | 18.2 | 21.6 |
| Reduction rate (%) | 10.04 | 10.46 | 11.18 | 9.70 | 10.93 | 11.75 | 5.71 | 6.99 | 12.0 | 11.00 | 11.3 | 12.33 |

occurs due to the closing of slat according to an increase in the surface solar radiation.

- As a result of analyzing the building energy consumption by applying the developed algorithm, building energy saving of up to 20.7 % in the cooling period and building energy saving of up to 12.3 % in the heating period were shown.
- When comparing the building energy saving performance according to the window-to-wall ratio for each orientation, the building energy saving effect for each orientation increased by up to approximately 70 % as the window-to-wall ratio increased in the cooling period, whereas the building energy saving effect in the heating period increased by approximately 50 %, indicating that the effects of window-to-wall ratio were higher in the cooling period.

**Acknowledgements** This work was supported by the National Research Foundation of Korea (NRF) Grant funded by the Korea government (Ministry of Science and ICT) (No. 2015R1A1A1A05000964).

## References

1. M.H. Oh, K.H. Lee, J.H. Yoon, Automated control strategies of inside venetian blind considering visual comfort and building energy performance. Energy Build. **55**, 728–37 (2012)
2. M.H. Oh, Jong-Ho Yoon, The effects of automatically controlled venetian blind to reflect optimum control strategies which are reducing discomfort-glare and improving energy performance. JAIK Plan. Des. **28**, 293 (2012)
3. H.B. Gunay, W. O'Brien, I. Beausoleil-Morrison, S. Gilani, Development and implementation of an adaptive lighting and blinds control algorithm. Build. Environ. **113**, 185–199 (2017)
4. G.M. Kang, K.N. Kang, D.S. Song, Optimized blind control method to minimize heating. Cool. Light. Energy Energy Procedia **78**, 2857–2862 (2015)
5. C. Zhijin, Z. Qianchuan, W. Fulin, J. Yi, X. Li, D. Jinlei, Satisfaction based Q-learning for integrated lighting and blind control. Energy Build. **127**, 43–55 (2016)
6. M.H. Oh, Optimum Automated Control Strategies of Inside Venetian Blind Considering Visual Comport and Building Energy Performance, Hanbat University, Master's Thesis (2012)
7. J. Hu, S. Olbina, Illuminance-based slat angle selection model for automated control of split blinds. Build. Environ. **46**, 786–796 (2011)
8. C.F. Reinhart, Lightswith-2002: a model for manual and automated control of electric lighting and blinds. Sol. Energy **77**, 15–28 (2004)
9. Y.J. Park, J.Y. Park, J.H. Kim, M.S. Yeo, K.W. Kim, An experimental study on environmental performance by the application of the automatic blind in summer. JAIK Plan. Des. **26**, 605–608 (2006)
10. The U.S. Department of Energy, EnergyPlus input output reference. The encyclopedic reference to EnergyPlus input and output (2010). http://www.energyplus.gov. Accessed 16 August 2017
11. K.H. Lee, Visual Comfort and Energy Characteristics Depending on Window Orientation for Optimized Slat Angle Control of Venetian Blind, Hanbat University, Master's Thesis (2017)
12. ASHRAE Fundamentals Handbook, American Society of Heating, Refrigerating and Air-Conditioning Engineers, Inc (2009)
13. The U.S. Department of Energy, EnergyPlus Engineering Reference. The Reference to EnergyPlus Calculations (2010). http://www.energyplus.gov. Accessed 16 August 2017
14. H.J. Kwon, K.H. Lee, K.H. Lee, Optimized slat angle control algorithm prediction of venetian blind depending on window orientation for energy saving. JKIEAE **17**, 99–106 (2017)
15. H.C. Yoo, S.H. Park, The review and evaluation of calculation methods for improving typical weather data of Seoul. JAIK Plan. Des. **28**, 265–274 (2012)
16. H.J. Kwon, K.H. Lee, K.H. Lee, Development and comparative analysis of slat angle control algorithm of venetian blind according to window-to-wall ratio and zone orientation. JKIEAE **17**, 75–81 (2017)
17. R.G. Hopkinson, Glare from daylighting in buildings. Appl. Ergon. **3**, 206–215 (1972)